Journal of Applied Physics ARTICLE pubs.aip.org/aip/jap

# Impurity stability based upon stress-corrected strain representation

Cite as: J. Appl. Phys. **137**, 135702 (2025); doi: 10.1063/5.0252446
Submitted: 9 December 2024 · Accepted: 18 March 2025 ·
Published Online: 2 April 2025

View Online Export Citation CrossMark

Hang Chen, Shengyuan Wang, and Junyi Zhu[a)]

## AFFILIATIONS

Department of Physics, The Chinese University of Hong Kong, Shatin, New Territories, Hong Kong, China

[a)]**Author to whom correspondence should be addressed:** jyzhu@phy.cuhk.edu.hk

## ABSTRACT

Using strain to control the formation energy or concentration of impurities, defects, and alloy components in semiconductors is crucial to improving their device functions. However, under small strains, existing studies on predicting impurity formation energy have three problems: incorrect strain representation due to inconsistency in the equilibrium state of the system before and after doping, incorrect stress sampling, and problems in the classification and analysis of stress introduced by impurities. To solve the above problems, we first define the volume ratio before and after doping in the equilibrium lattice. To obtain this volume ratio, we proposed a method to use the linear fitting of stress in a small strain range. Furthermore, we obtained the correct representation of strain before and after doping, and under this representation, we corrected the formula of impurity induced stress and formation energy under strains. Based on this theory, taking doped GaN and silicon as examples, we quantitatively studied impurity induced stress and formation energy under applied strain and found that the prediction accuracy was improved by about six times and four times, respectively, which confirmed the effectiveness of the strain correction formula. Based on the representation, we proposed a new method to estimate the size of dopants using fully compensated doping, thereby further classifying and analyzing the response mechanism of dopant induced stress to external strains. For substitutional impurities, this mechanism consists of the electron gas effect and the size effect; for nitrogen vacancy, there is a local coupling effect of dangling bonds of gallium atoms.





## I. INTRODUCTION

Predicting stresses and formation energies of impurities, defects, and alloy components in crystals under small strains is an important issue in semiconductor physics, because strain has been shown to change the impurity concentration or alloy ratio in various semiconductor systems.[1–3] The existing theoretical studies combine elastic mechanics and hydrogenic model.[4–13] However, these studies have the following three problems: (1) the difference between the equilibrium states of the system before and after doping leads to incorrect strain representation; (2) the potential problem in the estimation of formation energy if only the impurity induced stress at the equilibrium position is used; (3) an incomplete classification of the physical mechanism of this stress may affect our understanding of the response of formation energy to strain. Therefore, it is necessary for us to re-examine these issues.

Since the definition of strain depends on the reference state of the equilibrium position, and the equilibrium volume of the crystal before and after doping is different, there is a problem of aligning the reference state of strain in traditional predictions. Let us start with the setting of impurity formation energy calculation in a general sense. In this type of calculation, based on a supercell of the same volume, people take the difference between the energy before and after doping.[5] However, this standard method has a serious problem in the calculation of the relationship between formation energy and strain. Because the equilibrium volume changes after doping, the same strain corresponds to supercells of different volumes. Therefore, the doping calculations on supercell of the same volume will lead to errors in the strain estimation. Here, we take a simple one-dimensional chain as an example to show the difference in the length of the one-dimensional chain under the same strain caused by the difference between the equilibrium volumes, as shown in Fig. 1. Furthermore, because the equilibrium volume is related to the impurity concentration, the higher the impurity concentration, the greater the difference in equilibrium volume before and after doping, and the greater the error in strain estimation caused by supercells of the same volume. In summary,

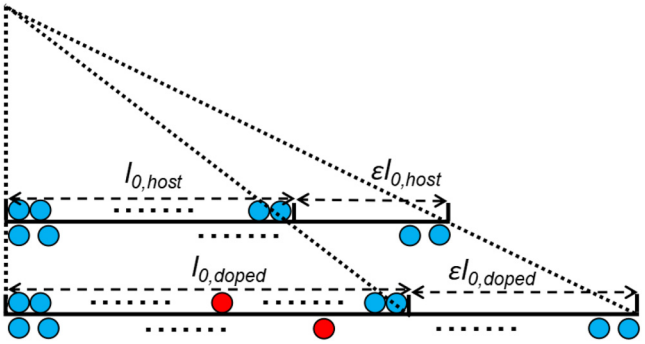


**FIG. 1.** Illustration of one-dimensional chain before and after doping under the same strain $\varepsilon$. $l_{0,host}$ and $l_{0,doped}$ are the equilibrium lengths of the one-dimensional chain before and after doping, respectively. $\varepsilon l_{host}$ and $\varepsilon l_{doped}$ are their respective length changes under deformation. The blue and red circles represent the host atoms and impurity atoms, respectively. The atoms above and below the line, respectively, represent the one-dimensional chain before and after applying the strain. The other atoms in the middle have been omitted. The dotted lines are to illustrate the proportional relationship between lengths.

the change in equilibrium volume before and after doping is very important for the representation of strain, so the errors in the traditional literature need to be corrected.

In addition, according to the energy integration formula of elastic theory, the traditional scheme also has the problem of selecting the stress introduced by impurities, which needs to be corrected. Based on the elastic theory, the impurity formation energy difference under hydrostatic strain $E_{R.E.}(\varepsilon)$ can be expressed as[8,14]

$$E_{R.E.}(\varepsilon) = \Omega_{0,\mathrm{host}} \int \sigma_{\mathrm{dopant}}(\varepsilon) d\varepsilon, \tag{1}$$

where $\Omega_{0,\mathrm{host}}$ is the equilibrium volume of the host crystal, $\varepsilon$ is the hydrostatic strain, and $\sigma_{\mathrm{dopant}}(\varepsilon)$ is the stress introduced by the impurity in the crystal after deformation. The previous approach used the stress induced by the impurity under the equilibrium volume of the host crystal $\sigma_{\mathrm{dopant}}(0)$ and the equilibrium volume calculated by density functional theory (DFT) to make an estimation.[8] However, $\sigma_{\mathrm{dopant}}(\varepsilon)$ can change significantly with the applied strain $\varepsilon$. In addition, when DFT calculates the equilibrium state before and after doping, the numerical error of its volume will also bring some additional stress, so the deviation of these stresses will lead to significant errors in energy prediction. A reasonable approach is to fit the impurity induced stress in a small strain range near the equilibrium position to obtain the correct strain representation, thereby improving the prediction accuracy of impurity induced stress and formation energy.

Additionally, there may be problems in classifying the physical mechanism of the response of impurity induced stress to external strain, and this problem may affect our understanding of the response mechanism of energy to external strain. In the traditional scheme, the stress introduced by impurities is considered to be a superposition of classical size effects and quantum electron gas effects.[5,7,15] The former can be estimated by the covalent bond radius of the atom; while the latter can be estimated by the electron gas assumption.[5,15] However, there is a lack of objective criteria for estimating covalent bond radius, as its accurate estimation requires eliminating the effects of different electronic environments. Here, we propose a new scheme to estimate the size effect, which is to calculate this part of the stress by adding or subtracting electrons from the impurity to form an electrically neutral doping configuration, details are given below. In addition, the stress caused by the electron gas can be accurately calculated by adding or subtracting electrons from the host lattice.[7] However, this classification is probably not applicable to vacancy-type impurities like nitrogen vacancy, because they will lead to local bond breaking and reconstruction of dangling bonds of atoms around the vacancy.[15–17] Therefore, the quantitative contribution of this physical mechanism to the stress should also be considered. However, traditional literature lacks a discussion on this aspect, and the only discussion related to vacancies mainly focuses on the formation energy.[8,9] However, if the estimate of the stress–strain response is not rigorous, the estimate of the formation energy-strain response cannot be correct. Therefore, once we are able to accurately estimate the contributions of the size effect and the electron gas model to the stress, the contribution of the reconstruction of atoms around the vacancy to the stress can be correctly revealed, and thus the mechanism that can be regulated by strain can be correctly expressed. Later, we will demonstrate this new classification and its effectiveness through specific examples.

In this article, because InGaN alloys, doped GaN, and silicon materials have important engineering significance, we use them as examples to study the changes in stress and formation energy under small strains. After correcting the error in the representation of external strain by fitting the stress near the equilibrium position, we made predictions for the stress and formation energy of $In_{Ga}$, p-type $Mg_{Ga}$, and n-type $V_N$ in GaN and compared them with the DFT-calculated values. We found that the prediction deviation of the new scheme is significantly smaller than that of the uncorrected scheme. Furthermore, we analyzed the physical mechanism of stress and classified it. Here, we selected the important $Mg_{Ga}$, $Ca_{Ga}$, nitrogen vacancies in GaN, and $B_{Si}$ and $P_{Si}$ in silicon. We found that regardless of the depth of the energy level, the stress caused by substitutional impurities under external strain can be accurately represented by the size effect and electron gas effect, while the stress caused by nitrogen vacancy has an additional effect on the response to external strain.

## II. METHODOLOGY

Total energy calculations based on DFT were implemented in the Vienna *Ab-initio* Simulation Package (VASP),[18,19] using a plane wave basis and strongly constrained and appropriately normed (SCAN) functional as the exchange-correlation functional,[20–23] because SCAN's prediction of lattice structure is more accurate than the prediction of generalized gradient approximation.[22,23] In the calculations, we used the standard supercell method. The GaN supercell has 96 atoms, with the x, y, and z directions corresponding to [2100], [0100], and [0001], respectively, and the lattice constants are 11.025, 9.558, and 10.374 Å, respectively. The Si supercell has 64 atoms, with the x, y, and z directions corresponding to

[100], [010], and [001], respectively, and the lattice constant is 10.870 Å. The plane wave cutoff energy we used was 550 eV, and the d electrons of In and Ga were explicitly included as valence electrons. For GaN and Si supercells, we sampled the Brillouin zone using $(3\times3\times4)$ and $(5\times5\times5)$ grids centered at the Γ point, respectively.[24] All atoms were relaxed until the force converged to less than 0.01 eV/Å. These calculation parameters were tested for convergence.

Under a small strain $\varepsilon$, the absolute formation energy of the impurity can be defined as[5,25]

$$E_f(\varepsilon) = E_{\text{doped}}(\varepsilon) - E_{\text{host}}(\varepsilon) + \mu_{\text{host}} - \mu_{\text{dopant}}, \tag{2}$$

where $E_{\text{host}}(\varepsilon)$ and $E_{\text{doped}}(\varepsilon)$ are the total energies of the system before and after doping, respectively, and $\mu$ is the chemical potential of one component in the growth environment. Further, referring to the absolute formation energy $E_f(0)$ at $\varepsilon = 0$, we can define the energy difference as relative formation energy $E_R(\varepsilon)$,

$$E_R(\varepsilon) = E_f(\varepsilon) - E_f(0) = E_{\text{doped}}(\varepsilon) - E_{\text{host}}(\varepsilon) - [E_{\text{doped}}(0) - E_{\text{host}}(0)]. \tag{3}$$

In order to avoid tedious discussion of chemical potential, in the subsequent results, we used the formation energy difference to describe the stability of impurities. In addition, the concept of small strain is relative, so we adopted the commonly used range of [−1.0%, 1.0%].[1–4] Beyond this small range, we also have some results around [−3.5%, 3.5%] to compare and highlight the unique behavior in the small strain range, which can be found in the supplementary material.

## III. RESULTS AND DISCUSSION

First, we corrected the strain deviation caused by the inconsistency of equilibrium state. Although the standard definition of strain, stress, and elastic constant in elastic theory are in tensor forms as stated in Ref. 26, in the context of hydrostatic stress that is isotropic, we only consider the diagonal terms of the tensor. For important conventional semiconductors, such as Si or GaN, the diagonal terms in elastic constant tensors are isotropic (for Si) or very close to be isotropic (for GaN);[27] therefore, we can approximate the strain tensor as a volumetric strain that is a scalar,

$$\varepsilon_v = \frac{\Omega - \Omega_0}{\Omega_0} = (1+\varepsilon_{xx})(1+\varepsilon_{yy})(1+\varepsilon_{zz}) - 1 \approx \varepsilon_{xx} + \varepsilon_{yy} + \varepsilon_{zz} = 3\varepsilon, \tag{4}$$

where $\Omega_0$ and $\Omega$ are the volumes before and after deformations, respectively, and here $\varepsilon_{xx} = \varepsilon_{yy} = \varepsilon_{zz} = \varepsilon$ (see supplementary material for details). Following this definition, we can define the volumetric strain for the host and doped system. When calculating the impurity formation energy, the crystal supercell before and after doping is usually set to the same volume. However, corresponding to the same volume, the strain before and after doping is different due to the difference in the equilibrium volume. In this way, when calculating the stress and formation energy after doping based on the same volume, there will be a slight difference between its actual strain and the actual strain of the host crystal. Specifically, referring to the equilibrium volume of the crystal before and after doping, we can define the actual hydrostatic strain before doping as follows:

$$\varepsilon = \frac{\Omega - \Omega_{0,\text{host}}}{3\Omega_{0,\text{host}}}, \tag{5}$$

and the actual strain after doping is defined as follows:

$$\varepsilon_d = \frac{\Omega - \Omega_{0,\text{doped}}}{3\Omega_{0,\text{doped}}}, \tag{6}$$

where $\Omega$ is the volume of the crystal after deformation and $\Omega_{0,\text{host}}$ and $\Omega_{0,\text{doped}}$ are their respective equilibrium volumes. Here, because the hydrostatic strain is isotropic, the three diagonal components of the strain tensor are identical. Therefore, according to Eq. (4), a ratio of 1/3 appears in Eq. (5) and (6). If only the equilibrium volume calculated by DFT is used, formulas (5) and (6) give the uncorrected strain in the DFT calculations. Since DFT calculations usually have a certain numerical deviation in the equilibrium volume, the calculated value of the strain may also have a certain deviation, which can be corrected by linear fitting of stress and strain. Based on this corrected strain, we respectively define the deviation of the strain before and after doping as

$$\Delta\varepsilon_h = \varepsilon - \varepsilon_h', \tag{7}$$

$$\Delta\varepsilon_d = \varepsilon_d - \varepsilon_d'. \tag{8}$$

Here, $\varepsilon_h'$ and $\varepsilon_d'$ correspond to the uncorrected calculated strains before and after doping, respectively.

For convenience, we erase the subscript $h$ of the actual strain of the host lattice. In addition, using the same volume, we can relate these two actual strains as follows:

$$\varepsilon_d = \eta\varepsilon - \frac{1}{3}(1-\eta), \tag{9}$$

where $\eta = \frac{\Omega_{0,\text{host}}}{\Omega_{0,\text{doped}}}$ is the ratio of the equilibrium volume of the crystal before and after doping after correcting the numerical error in volume. If the problem of inconsistency in the equilibrium state is not considered, the volume ratio $\eta = 1$. Furthermore, according to formula (9), we can also define the difference between the two actual strains,

$$\text{diff}_{(h-d)} = \varepsilon_d - \varepsilon = (\eta-1)\varepsilon - \frac{1}{3}(1-\eta), \tag{10}$$

For different impurities, this strain difference is varied. Since the two strains are related, here, for simplicity, we use the actual host strain $\varepsilon$ as the independent variable to estimate the stress and energy before and after doping.

Based on the above correction principles, we can further correct the equilibrium state before and after doping in the DFT calculations by linear fitting of stress under different strains. First, based on DFT, we automatically relax the unit cell and atomic

position of the host crystal to obtain a relatively rough equilibrium volume and its corresponding stress. Then, based on this rough equilibrium state, we apply a strain every 0.5% in the interval [−1.0%, 1.0%], calculate its stress, and make a linear fit for these five points. Among them, the slope of the fitted line is the elastic coefficient of the system, the intercept can be defined as the residual stress, and the equilibrium state corresponds to zero stress. According to the ratio of residual stress and elastic coefficient, we get the strain deviation. Substituting the strain deviation back into formulas (5) and (7), we can get the corrected equilibrium volume. Similarly, for doped crystals, we can also make similar corrections. The above fitting parameters are shown in Table I, and the original DFT calculation results and more fitting details are shown in the supplementary material. According to Table I, there is a certain difference between the host strain before and after correction, with a deviation of −0.040%, so the actual host strain interval is [−1.040%, 0.960%]. More importantly, due to the equilibrium volume change introduced by impurities, there is also a certain difference between the two actual strains before and after doping. The strain differences corresponding to $In_{Ga}$, $Mg_{Ga}$, and $V_N$ doping are −0.225%, −0.077%, and 0.040%, respectively, which illustrates the necessity of introducing strain correction after doping.

Next, based on the correction of the equilibrium state, we can predict the stress before and after doping and the stress introduced by impurities within a certain strain range. First, according to the elastic theory, the stress and actual strain before and after doping are proportional, so the stresses can be expressed, respectively, as

$$\sigma_{\text{host}} = k_h \varepsilon, \tag{11}$$

$$\sigma_{\text{doped}} = k_d \varepsilon_d, \tag{12}$$

where $k_h$ and $k_d$ are the fitted elastic coefficients of the crystal before and after doping, respectively (see supplementary material for details). Taking the actual strain $\varepsilon$ of the host crystal as the independent variable and combining formula (9), the stress after doping can be expressed as

$$\sigma_{\text{doped}} = \eta k_d \varepsilon - \frac{1}{3}(1-\eta)k_d. \tag{13}$$

If we do not consider the inconsistency of the equilibrium volume before and after doping, that is, $\eta = 1$, ignore the strain difference between the two, then formula (13) will become formula (12), and we can get the prediction results of the uncorrected strain scheme. In addition, we can regard formula (13) as a function of $\eta$, $\sigma_{\text{doped}}(\eta)$, then based on this function, we can roughly define the stress difference caused by whether to consider strain correction or not as

$$\begin{aligned}\Delta\sigma_{\text{doped}} &= \sigma_{\text{doped}}(\eta) - \sigma_{\text{doped}}(1) \\ &= k_d(\eta-1)\left(\varepsilon + \frac{1}{3}\right).\end{aligned} \tag{14}$$

It can be seen that the larger the volume and elastic coefficient introduced by the impurities, the greater the impact of not making the equilibrium volume correction on the stress prediction. According to Table I, this correction should have the greatest effect on indium doping. From formulas (13) and (14), we found that the equilibrium volume ratio $\eta$ is an important parameter for impurities, and this ratio will be different under different impurity concentrations, so the impurity concentration itself will also affect the magnitude of the stress after doping. Further, the stress introduced by impurities is defined as

$$\sigma_{\text{dopant}}(\varepsilon) = \sigma_{\text{doped}}(\varepsilon) - \sigma_{\text{host}}(\varepsilon). \tag{15}$$

Therefore, combining formulas (11), (13), and (15), our predicted value of the dopant induced stress can be expressed as

$$\sigma_{\text{dopant}}(\varepsilon) = (\eta k_d - k_h)\varepsilon - \frac{1}{3}(1-\eta)k_d. \tag{16}$$

The impurity induced stress here includes two parts of correction. One part is the strain correction caused by the inconsistency of the equilibrium volume before and after doping, and the other part is the numerical correction of the equilibrium volume of the host crystal. In the strain correction scheme, combining Table I and equations (11), (13), and (16), we can predict the response of the lattice stress before and after doping and the stress introduced by impurities to the actual strain of the host crystal.

In order to demonstrate the effectiveness of strain correction for stress prediction, we took the stress calculated by DFT as the true value and compared the deviations of the two schemes with and without strain correction. First, we took points every 0.2% in the interval [−1.040%, 0.960%] to test the prediction accuracy of the above scheme within the fitting interval. Specifically, we calculated the DFT stress of the host and the system doped with $In_{Ga}$, $Mg_{Ga}$, and $V_N$ and used this as a benchmark to compare the deviations of the above two prediction schemes (see the supplementary material for the specific definition of deviation), and the results are shown in Fig. 2(a). We can see that after strain correction, the stresses have all been corrected to a certain extent compared with the uncorrected scheme. Among them, for the cases of host and indium doping, the strain correction scheme corrects their stresses particularly significantly. For the host, this may be because while the equilibrium point is corrected, the deviation caused by the nonlinear effect of the lattice stress itself is also corrected by our linear fit. For the $In_{Ga}$ doped crystals, as mentioned above, because the $\eta$ and elastic coefficient introduced by indium atoms are the largest, the correction effect is the most obvious. Next, using the difference in lattice stress, we also estimated the response of the stress introduced by the three impurities under different strains, as shown in Fig. 2(b). We can see that in the interval [−1.040%, 0.960%], the stress introduced by impurities changes roughly linearly. Among them, for the $V_N$, the sign of the stress changes; for the $Mg_{Ga}$, the stress remains roughly unchanged. Therefore, for the $V_N$ and $In_{Ga}$ doping, if only the impurity stress at the equilibrium position is used, it will lead to a relatively large deviation in the prediction of the formation energy. So early proposal on the formation energy fitting is problematic because only equilibrium stress is taken into account.[8] Finally, taking the DFT-calculated values as true values, we also compared the deviations of the dopant induced stress

**TABLE I.** Fitted elastic constant, strain deviation, strain difference at the equilibrium $\varepsilon = 0$, equilibrium volume, and equilibrium volume ratio in the strain-corrected scheme.

| Type | Elastic constant (eV/Å$^3$) | Strain deviation (%) | Strain difference (%) | Equilibrium volume (Å$^3$) | Equilibrium volume ratio |
|---|---|---|---|---|---|
| Undoped | 10.9274 | −0.040 | ⋯ | 1094.61 | ⋯ |
| $In_{Ga}$ doped | 11.3505 | −0.035 | −0.225 | 1102.04 | 0.9933 |
| $Mg_{Ga}$ doped | 10.9343 | −0.032 | −0.077 | 1097.13 | 0.9977 |
| $V_N$ doped | 10.2995 | −0.038 | 0.040 | 1093.29 | 1.0012 |

under these two schemes, and the results are shown in Fig. 2(c). Compared with the uncorrected strain scheme, the predicted values of the strain-corrected scheme are closer to the true values, and its average deviation is reduced by six times. Specifically, the correction scheme is particularly successful for magnesium atoms and nitrogen vacancies. This may be because when we calculate the stress caused by indium atoms, the stress correction effects of the host crystal and the doped crystal are partially canceled, and this cancellation is not obvious in the cases of $Mg_{Ga}$ and $V_N$, as shown in Fig. 2(a) and formula (16). To further highlight the impact of the correction, we also calculated the percentage prediction deviation of impurity induced stress. For example, for the three types of impurities, at the two actual strains of −1.040% and −0.040%, the average percentage prediction deviations in the strain-corrected scheme are 5.3% and 4.0%, respectively, compared to 48.3% and 40.7% in the strain-uncorrected scheme. In addition, we can also test the prediction accuracy of the above scheme outside the fitting interval. Taking the interval [−2.040%, 1.960%] as an example, the average deviation of the dopant induced stress predicted by the corrected scheme increases slightly, 0.9 meV/Å$^3$, but it is still smaller than the uncorrected 3.3 meV/Å$^3$. This shows that the strain correction scheme can also make more accurate predictions outside the fitting interval. In summary, after correcting the errors in the strain representation in the traditional scheme, we obtained the correct strain representation, and based on this representation, our scheme significantly improved the prediction accuracy of stress caused by impurities.

Similar to the correction of stress, we can use the corrected strain to correct the impurity formation energy and compare it with the scheme without the corrected strain. When correcting, we substitute the stress introduced by impurities, that is, formula (16), into formula (1) and integrate it, then the impurity formation energy is

$$E_{R.E.}(\varepsilon) = \Omega_{0,\mathrm{host}}\left[\frac{1}{2}(\eta k_d - k_h)\varepsilon^2 - \frac{1}{3}(1-\eta)k_d\varepsilon\right]. \quad (17)$$

For different impurities, due to the differences in equilibrium volume ratio and elastic coefficient before and after doping, their formation energy responds differently to strain. In addition, we can regard formula (17) as a function of $\eta$, $E_{R.E.}(\eta)$. Correspondingly,



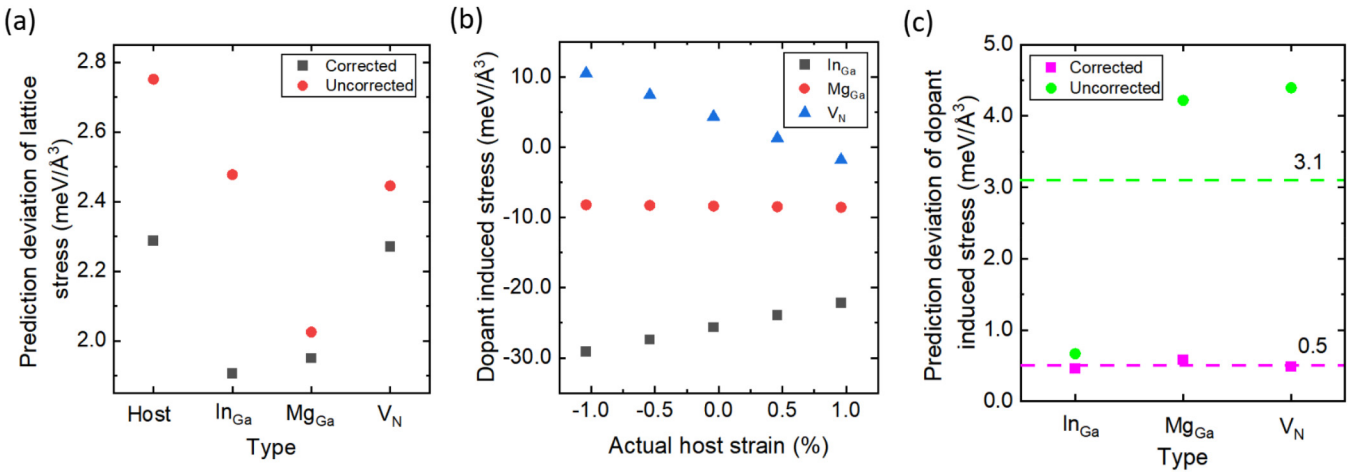


**FIG. 2.** (a) Prediction deviation of lattice stress given by the strain-corrected scheme and the strain-uncorrected scheme. The black and red points correspond to the deviation in the corrected scheme and the uncorrected scheme, respectively. (b) Changes of dopant induced stress estimated by the corrected scheme with the corrected actual host strain. The black, red, and blue points correspond to the cases of $In_{Ga}$, $Mg_{Ga}$, and nitrogen vacancy, respectively. (c) Comparison of the prediction deviation of dopant induced stress given by the corrected scheme and the uncorrected scheme. The purple and green points correspond to the cases of the corrected scheme and the uncorrected scheme, respectively. The purple and green dashed lines, respectively, show their average prediction deviations.

when the strain is not corrected, that is, $\eta = 1$, we can obtain the uncorrected impurity formation energy. In this way, we can roughly define the deviation of impurity formation energy caused by considering strain correction as

$$\Delta E_{R.E.}(\eta) = E_{R.E.}(\eta) - E_{R.E.}(1) = \Omega_{0,\text{host}} k_d (\eta - 1)\left(\frac{1}{2}\varepsilon^2 + \frac{1}{3}\varepsilon\right). \quad (18)$$

It can be seen that the deviation has a nonlinear response to strain, and the larger the strain, the more significant the nonlinear response. Substituting the data in Table I into formulas (17) and (18), we can obtain the impurity formation energy with and without correction and the deviation. Also, our findings lay a solid foundation for future studies in large strain affected stress and formation energy, which is beyond the scope of this paper.

Next, we used the formation energy calculated by DFT as the ground truth and compared the average absolute deviation of the two schemes with and without strain correction. In the formation energy calculations, we first calculated the relative one in reference to the undeformed host lattice without the strain correction. Then, we corrected the strain representation following the stress fitting results, as shown in Fig. 3(a). Specifically, we first estimated the formation energy of three impurities, $In_{Ga}$, $Mg_{Ga}$, and $V_N$, in the interval [−1.040%, 0.960%] according to formula (17). We can see that the impurity formation energy changes roughly linearly. Among them, as the strain increases, the formation energy of indium atoms and magnesium atoms gradually decreases, while the formation energy of nitrogen vacancies gradually increases. It is worth noting that as the strain increases, the formation of nitrogen vacancies can show a nonlinear response. To understand it, we need to correctly classify and understand the physical mechanism of stress introduced by impurities, which will be discussed later. Then, we set $\eta$ to 1, calculated the formation energy under the strain-uncorrected scheme, and then used the DFT-calculated value as the ground truth to compare the prediction accuracy of the two schemes, and the results are shown in Fig. 3(b). For these three impurities, the average absolute deviation of the corrected scheme is within 5.0 meV, while the deviation of the uncorrected scheme is two to five times that of the corrected scheme. This shows that under very small strains, the strain correction scheme can still effectively reduce the prediction deviation. In addition, we estimated the formation energy outside the fitting interval. In the interval [−2.040%, 1.960%], the deviation of the strain correction scheme is within 10.0 meV, and the average absolute deviation of the corrected scheme is about twice smaller than that of the uncorrected scheme. This shows that the correction scheme can also make accurate predictions of the formation energy outside the fitting interval. Additionally, there is a scheme that proposes to predict the impurity formation energy using only the stress introduced by the impurities at the equilibrium position and the uncorrected strain. We also calculated the predictions and deviations of this scheme, and the results showed that the average deviations of this scheme were two and five times that of the corrected scheme within and outside the fitting interval, respectively. In summary, after correcting the problems of strain representation and dopant induced stress, we can obtain accurate predictions of impurity formation energies both inside and outside the fitting interval.

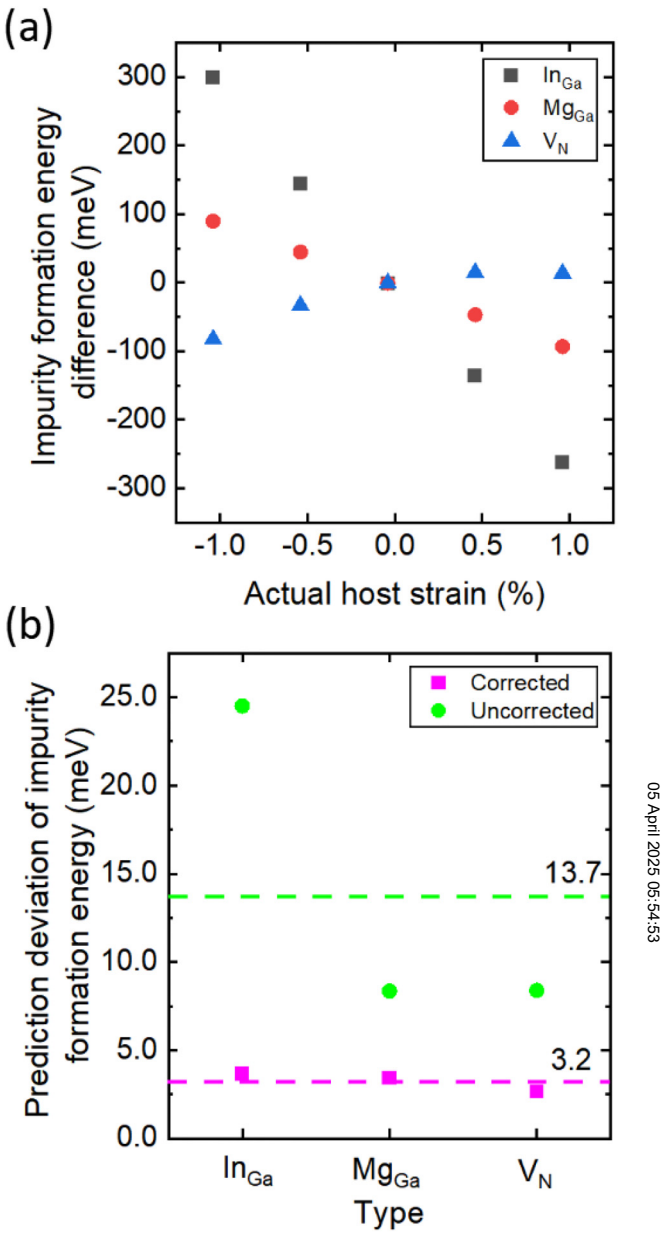


**FIG. 3.** (a) Changes of impurity formation energy difference estimated by the scheme with the corrected actual host strain. The black, red, and blue points correspond to the cases of $In_{Ga}$, $Mg_{Ga}$, and nitrogen vacancy, respectively. (b) Prediction deviation of the impurity formation energy. The purple and green points correspond to the cases of the corrected scheme and the uncorrected scheme, respectively.

Furthermore, we can analyze the response mechanism of dopant induced stress under external strain and extend this analysis

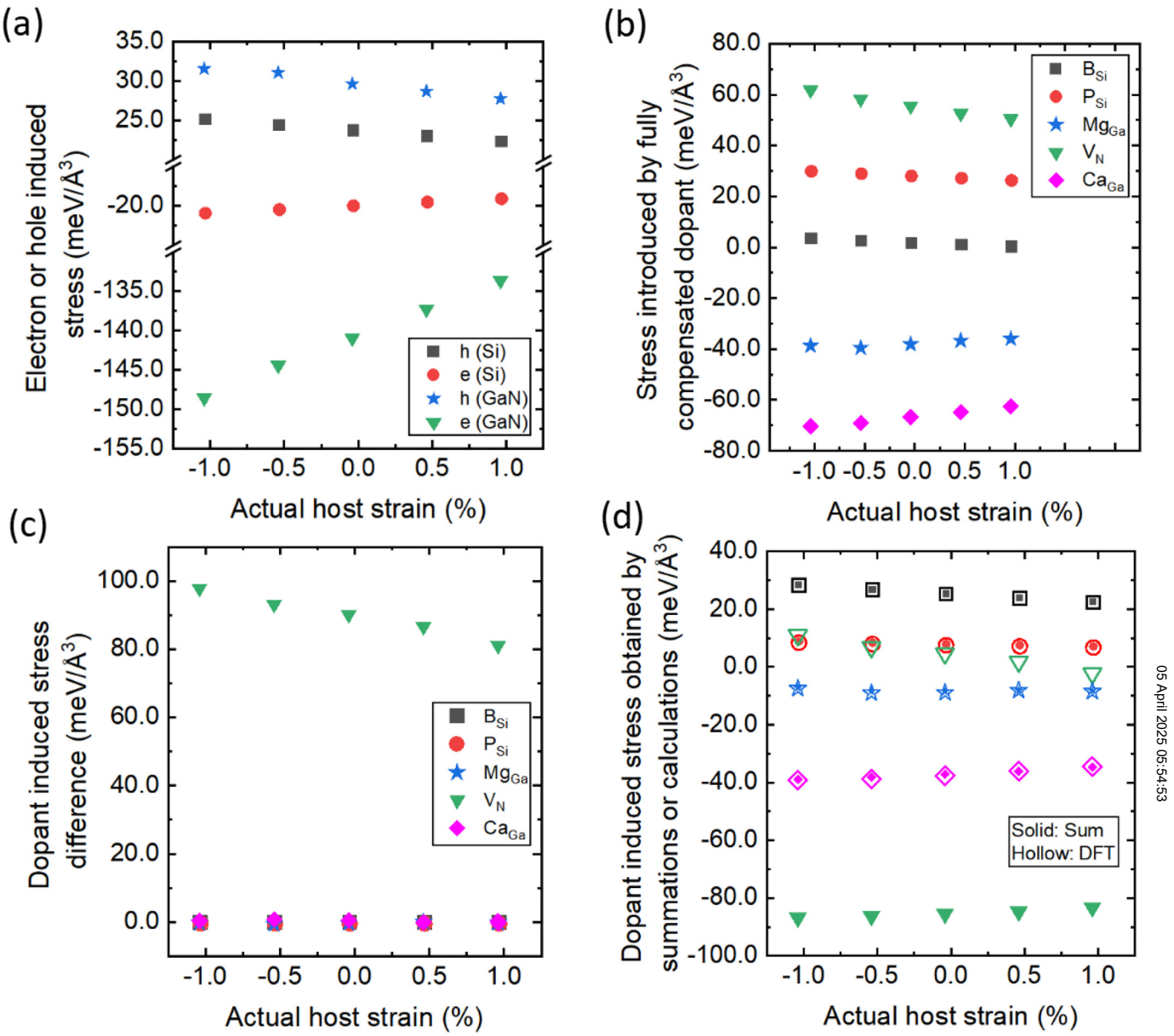


**FIG. 4.** (a) Electron or hole induced stress as a function of external strain. The black, red, blue, and green points represent the introduction of one hole and one electron in silicon and one hole and three electrons in GaN, respectively. (b) Stress introduced by fully compensated dopant as a function of external strain. (c) The difference between the summed dopant induced stress and the DFT-calculated dopant induced stress. (d) Dopant induced stress obtained by summations or DFT calculations as a function of external strain. Among (b), (c), and (d), the black, red, blue, purple, and green points correspond to $B_{Si}$ and $P_{Si}$ in silicon, $Mg_{Ga}$, $Ca_{Ga}$, and nitrogen vacancy in GaN, respectively. Specifically, in (d), the solid points represent summed stresses, and the hollow points represent DFT-calculated stresses.

to silicon systems. First, we can study the response introduced by the electron gas effect. Quantitatively speaking, under external strain [−1.040%, 0.960%], we can calculate the stress of the electron gas by adding or subtracting electrons from the host crystal. For the electron gas response of $Mg_{Ga}$ and $Ca_{Ga}$, we can calculate it by subtracting one electron from the GaN host lattice; and for $V_N$, similarly, we can calculate it by adding three electrons. In addition, we extended this algorithm to the silicon system and calculated the stress response of silicon after adding or subtracting one electron, and the results are summarized in Fig. 4(a). It is worth noting that the strain correction

of silicon is slightly different from that of GaN, and its strain range is [−1.033%, 0.967%]. We can see that in these four doping cases, the stress introduced by the electron gas effect responds roughly linearly to the external strain, and for electron doping, its slope is positive, while the slope for holes is negative.

Similarly, we also studied the response of the stress introduced by the impurity size effect to the external strain. To calculate this stress, we can add or subtract electrons from the impurity to form an electrically neutral doping configuration. It is worth noting that early literature lacked an effective calculation method for the size effect, and researchers usually estimated the size effect by taking an empirical covalent bond radius.[28] Here, we list the results of DFT calculations, as shown in Fig. 4(b). We can see that in these five doping cases, the stress introduced by the size effect also responds roughly linearly to the external strain. Moreover, for $Mg_{Ga}$ and $Ca_{Ga}$, which introduce crystal expansion, the slope is positive; while for $B_{Si}$, $P_{Si}$, and $V_N$, which introduce volume contraction, the slope is negative. This is consistent with the description of the empirical covalent bond radius, that is, the radii of Mg and Ca are larger than that of Ga, while the radii of B and P atoms are smaller than that of Si.[28] Of course, the correctness of our new calculation method still needs to be confirmed by whether the sum of the two stresses matches the total stress of the defect.

Whether the sum of the stresses caused by the above two effects matches the overall dopant induced stress is an interesting physical question. Based on the results of Figs. 4(a) and 4(b), we obtained the sum of the stresses of the two effects. Next, referring to the dopant induced stress calculated by DFT, we can obtain the difference between the two, as shown in Fig. 4(c). We can see that for substitutional impurities, $B_{Si}$ and $P_{Si}$ in silicon and $Mg_{Ga}$ and $Ca_{Ga}$ in GaN, the difference in dopant induced stress is almost zero, that is, the sum of the stresses caused by the two effects matches the overall dopant induced stress. However, for $V_N$ in GaN, the dopant induced stress difference is obviously not zero, and it responds roughly linearly to external strain, because the nitrogen vacancy can lead to localized bond breaking and significant reconstructions of gallium atoms around the vacancy. But when the three electrons are removed from the system, there are no electrons on the dangling bonds of these gallium atoms, thus creating a significant repulsion, which increases the distance between gallium atoms by approximately 20%, the local structures are shown in the supplementary material. This additional highly localized coupling between gallium atoms cannot be effectively described by the electron gas model. Of course, whether all vacancy defects respond similarly requires further study and is beyond the scope of this article. Additionally, we also extended the study to a large strain range near [−2.0%, 2.0%] and observed approximate linearity for all substitutional dopants (see supplementary material for details). In summary, the electrically neutral doping configuration is a model that can correctly express the size effect of substitutional impurities. This model combined with the stress introduced by electron gas can obtain the total stress of substitutional impurities. In addition, the difference in this stress can also be used to characterize the response of the local coupling of the dangling bonds of Ga atoms near nitrogen vacancies to external strain.

In addition to the stress response, we finally summarize the response of formation energy in these two doping systems.

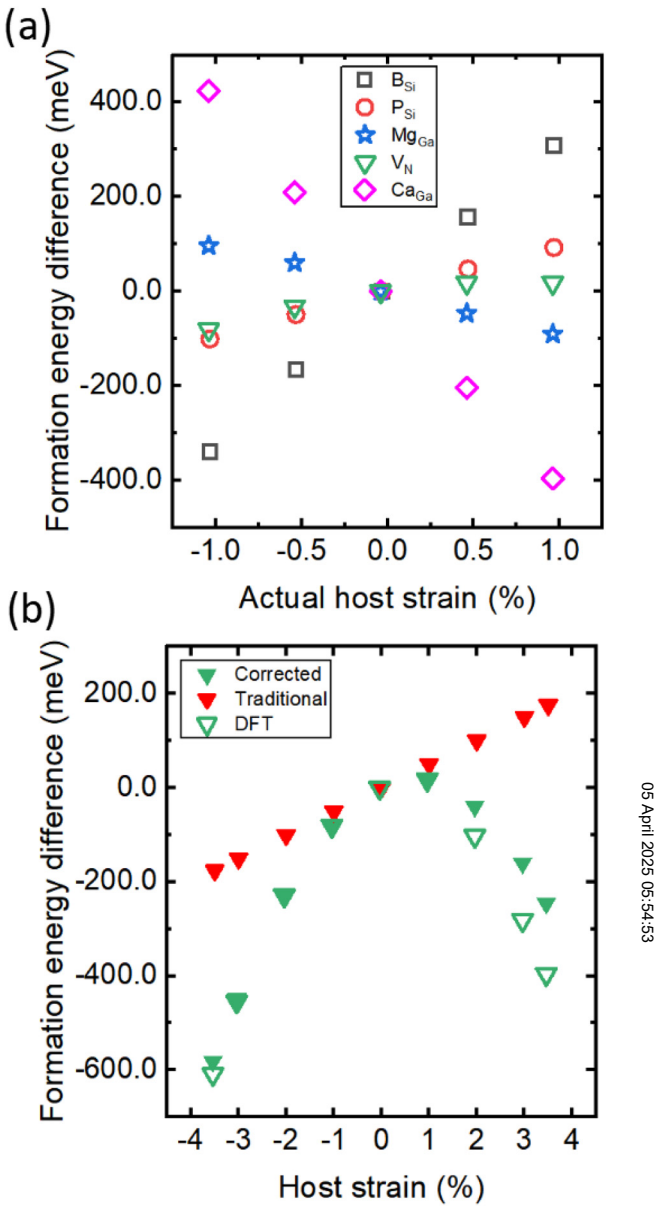


**FIG. 5.** (a) Changes of impurity formation energy difference calculated by DFT as a function of their respective actual host strains. The black, red, blue, purple, and green hollow points correspond to $B_{Si}$ and $P_{Si}$ in silicon, $Mg_{Ga}$, $Ca_{Ga}$, and nitrogen vacancy in GaN, respectively. (b) Changes in formation energy difference of nitrogen vacancy calculated by DFT, the corrected scheme, and the traditional scheme. The green hollow points, green solid points, and red points correspond to the results of DFT, the corrected scheme, and the traditional scheme, respectively.

According to Fig. 4(d), for $P_{Si}$, $B_{Si}$, $Mg_{Ga}$, and $Ca_{Ga}$, we can see that the slope of their stress is close to zero, and the energy difference with reference to the equilibrium position is roughly linear, as shown in Fig. 5(a). However, if the slope of the stress is relatively

large, this energy difference will express significant nonlinearity, as shown in $V_N$ in Fig. 5(a). We noticed that the slope of the stress caused by the size effect and the electronic effect of $V_N$ is relatively small, so the nonlinearity of its formation energy difference mainly comes from its vacancy characteristics. However, this does not mean that the nonlinear response of the formation energy difference must be caused by vacancies. For example, the slope of the stress introduced by $In_{Ga}$ is also relatively large, so its energy response also has a certain nonlinear contribution. Finally, when we take into account the size effect, electron gas effect, and local response of nitrogen vacancies, since their respective equilibrium volumes are significantly different, there will also be certain nonlinear effects on the formation energy under the representation of strain. These new findings show that the response of the electron gas is a universal effect, while the size and local response are related to the physical properties of the impurity itself. This understanding also lays the foundation for simply and effectively fitting the response of various types of impurities to strain, and for studying the response of impurity induced stress and formation energy under larger strains. To show the potential applications of these modifications, including those for strain and stress, it is essential to compare them with the traditional scheme where no corrections were applied as stated in Ref. 8. Taking $V_N$ impurity in GaN as an example, we extend the comparison to a large strain range of [−3.540%, 3.540%], with the results shown in Fig. 5(b). It can be observed that the predictions of the corrected scheme are much more accurate than those of the traditional scheme. At the large strains of −3.540% and 3.540%, the corrected scheme largely reduces the deviations to about 6.2% and 26.3% of the traditional one, respectively. At a typical growth temperature of 1000 K, our scheme leads to significant corrections of the formation energy at these two strain conditions for about 400 meV, which results in a correction on the nitrogen vacancy concentration for about two orders of magnitude higher than the uncorrected case. As a result, our new scheme will also largely correct the transition energy results, which are also based on the formation energy. In addition, the transition energy corrections will also lead to improved predictions in charge transport and device simulations for stressed devices that are critical in the semiconductor industry. For highly anisotropic systems, the volumetric strain still should follow the tensor form, which is beyond the scope of this paper, but the general treatment on the different equilibrium volumes for the host and doped system should be applied as well.

## IV. CONCLUSIONS

In general, in the study of the influence of strain on impurity induced stress and impurity formation energy, we corrected the inconsistency error in the representation of strain in the doping system and the host crystal. In addition, we defined a volume ratio of the equilibrium lattice before and after doping to conveniently predict the dopant induced stress and formation energy of the dopant, suggesting that the stress and energy are concentration dependent. The strain correction and volume ratio can be calculated by linearly fitting the stress as a function of strain near the range of [−1.0% to 1.0%]. Then, we took doped GaN and silicon bulk materials as examples and proposed a simple prediction method of dopant induced stress and formation energy and significantly improves the prediction accuracy by six times and four times, respectively. An accurate prediction for substitutional dopants near the range of [−2.0%, 2.0%] was also achieved. Based on this correct prediction method, we proposed the concept of fully compensated dopants and used it to characterize the size contribution of the response of dopant induced stress to the external strain. Combined with the electron gas contribution of this response, we can accurately describe the response of stress introduced by substitutional dopant to external strain. In addition, we also found that nitrogen vacancy has additional local coupling responses to external strain. Based on these findings, we can quantitatively classify and analyze the response of dopants to external strain.

## SUPPLEMENTARY MATERIAL

See the supplementary material for definition of small strain, derivation of actual strain definition, correction scheme for lattice strain, definition of prediction deviation, comparison of $Ca_{Ga}$ and $V_N$ impurity-related local structures, and response of dopant induced stress under large strains.

## ACKNOWLEDGMENTS

We acknowledge the Innovation Program for Quantum Science and Technology (Project No. 2023ZD0300600), the General Research Fund (No. 14304624) from Research Grants Council in Hong Kong, the Young Collaborative Research Grant (C4005-22Y), and the SIAT-CUHK Joint Laboratory of Photovoltaic Solar Energy for research fund.



## AUTHOR DECLARATIONS

### Conflict of Interest

The authors have no conflicts to disclose.

### Author Contributions

**Hang Chen:** Data curation (lead); Formal analysis (equal); Investigation (equal); Methodology (equal); Writing – original draft (equal); Writing – review & editing (equal). **Shengyuan Wang:** Methodology (supporting); Writing – review & editing (supporting). **Junyi Zhu:** Conceptualization (lead); Formal analysis (equal); Investigation (equal); Methodology (equal); Project administration (lead); Supervision (lead); Writing – original draft (equal); Writing – review & editing (equal).

## DATA AVAILABILITY

The data that support the findings of this study are available from the corresponding author upon reasonable request.

## REFERENCES

[1]T. Ikuta, Y. Miyanami, S. Fujita, H. Iwamoto, S. Kadomura, T. Shimura, H. Watanabe, and K. Yasutake, Jpn. J. Appl. Phys. **46**(4S), 1916 (2007).
[2]N. S. Bennett, A. J. Smith, R. M. Gwilliam, R. P. Webb, B. J. Sealy, N. E. B. Cowern, L. O'Reilly, and P. J. McNally, J. Vac. Sci. Technol. B **26**(1), 391 (2008).

[3]W. Jiao, W. Kong, J. Li, K. Collar, T.-H. Kim, and A. S. Brown, Appl. Phys. Lett. **103**(16), 162102 (2013).
[4]C. Ahn, N. Bennett, S. T. Dunham, and N. E. B. Cowern, Phys. Rev. B **79**(7), 073201 (2009).
[5]J. Zhu, F. Liu, G. B. Stringfellow, and S.-H. Wei, Phys. Rev. Lett. **105**(19), 195503 (2010).
[6]Z. Wang, S. Chen, X. Duan, D. Sun, and X. Gong, J. Phys. Soc. Jpn. **81**(7), 074712 (2012).
[7]H. Hu, M. Liu, Z. F. Wang, J. Zhu, D. Wu, H. Ding, Z. Liu, and F. Liu, Phys. Rev. Lett. **109**, 055501 (2012).
[8]J. Zhu, F. Liu, and M. A. Scarpulla, APL Mater. **2**(1), 012110 (2014).
[9]X. Yan, P. Li, S.-H. Wei, and B. Huang, Chin. Phys. Lett. **38**(8), 087103 (2021).
[10]I. Kim, H. Lee, and M. Choi, J. Appl. Phys. **131**(7), 075106 (2022).
[11]M. Lan, R. Wang, Y. Song, and S.-H. Wei, J. Appl. Phys. **134**(4), 045703 (2023).
[12]W. Li, W. Liu, Y. Liang, X. Liu, Y. Xu, X. Wu, C.-L. Yang, and C. S. Liu, Comput. Mater. Sci. **231**, 112564 (2024).
[13]J. Zhang, L. Guan, Z. Chen, T. Luo, T. Yin, X. Ren, W. Shi, C. Liu, X. Chen, and X. Li, Appl. Surf. Sci. **679**, 161235 (2025).
[14]U. M. E. Christmas, D. A. Faux, and N. E. B. Cowern, Phys. Rev. B **76**(20), 205205 (2007).
[15]Y. U. Peter and M. Cardona, *Fundamentals of Semiconductors: Physics and Materials Properties* (Springer, Berlin 2010), p. 161.
[16]J. Neugebauer and C. G. Van de Walle, Phys. Rev. Lett. **75**(24), 4452 (1995).
[17]W. A. Harrison, *Elementary Electronic Structure* (World Scientific, 2004), p. 313.
[18]G. Kresse and J. Furthmüller, Comput. Mater. Sci. **6**(1), 15 (1996).
[19]G. Kresse and J. Hafner, Phys. Rev. B **49**(20), 14251 (1994).
[20]G. Kresse and D. Joubert, Phys. Rev. B **59**(3), 1758 (1999).
[21]P. E. Blöchl, Phys. Rev. B **50**(24), 17953 (1994).
[22]J. Sun, A. Ruzsinszky, and J. Perdew, Phys. Rev. Lett. **115**(3), 036402 (2015).
[23]J. Sun, R. C. Remsing, Y. Zhang, Z. Sun, A. Ruzsinszky, H. Peng, Z. Yang, A. Paul, U. Waghmare, X. Wu, M. L. Klein, and J. P. Perdew, Nat. Chem. **8**(9), 831 (2016).
[24]H. J. Monkhorst and J. D. Pack, Phys. Rev. B **13**(12), 5188 (1976).
[25]S. H. Wei, Comput. Mater. Sci. **30**(3–4), 337 (2004).
[26]L. D. Landau, L. P. Pitaevskii, A. M. Kosevich, and E. M. Lifshitz, *Theory of Elasticity: Volume 7* (Butterworth-Heinemann, 2012), p. 3.
[27]H. Fukuda, A. Nagakubo, S. Usami, M. Imanishi, Y. Mori, and H. Ogi, Appl. Phys. Express **17**, 016501 (2024).
[28]J. A. Van Vechten and J. C. Phillips, Phys. Rev. B **2**(6), 2160 (1970).

# Supplementary Material for "Impurity Stability Based upon Stress-Corrected Strain Representation"

Hang Chen, Shengyuan Wang, and Junyi Zhu[a)]

*Department of Physics, The Chinese University of Hong Kong, Shatin, New Territories, Hong Kong, China*

## 1. Definition of small strain

The definition of small strain is relative and lacks a universally accepted range. To address this, we adopted the frequently used range of small strain, around [-1.0%, 1.0%], in traditional literature.[1-4] In this range, the impurity formation energy exhibits an approximately linear response to the applied external strain. In addition, to further clarify the effect of strain beyond this range, we have performed additional impurity formation energy calculations at larger strains of [-3.5%, 3.5%]. Under the whole range of [-3.5%, 3.5%], the impurity formation energies show a nonlinear response to the external strain, as shown in FIG. S1. The linear response of the impurity formation energy to small strain can be used as a characteristic of small strain.

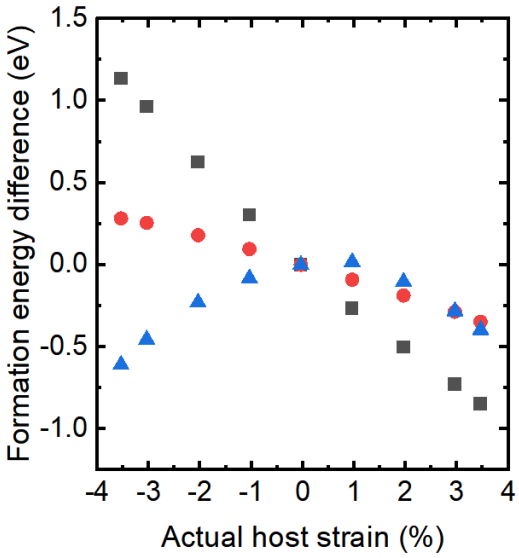


FIG. S1. Changes of impurity formation energy difference calculated by DFT as a function of their respective actual host strains. The black, red, and blue points correspond to the cases of $In_{Ga}$, $Mg_{Ga}$, and nitrogen vacancy in GaN, respectively.

[a)] jyzhu@phy.cuhk.edu.hk

## 2. Derivation of actual strain definition

The definitions of actual strains can be derived from the standard strain definition in the elasticity theory under small, isotropic, and hydrostatic strains. Firstly, for the standard definition in elasticity theory as outlined by L. D. Landau et al. (2012),[5] this strain tensor provides the most general framework for describing deformation, capturing both normal and shear components. For any point in a body under small deformations, it is defined as,[5]

$$\varepsilon_{ij} = \frac{1}{2}\left(\frac{\partial u_i}{\partial x_j} + \frac{\partial u_j}{\partial x_i}\right) \quad \text{(S1)}$$

, where $u_i$ is the displacement component of the point in the $i$ direction, $x_j$ is the point position in the $j$ direction. Secondly, to describe deformations in a single direction, we can define linear strain as the diagonal component of the strain tensor,[6]

$$\varepsilon_{ii} = \frac{\partial u_i}{\partial x_i} \approx \frac{u_i}{x_i} = \frac{\Delta L_i}{L_i} \quad \text{(S2)}$$

, where $\varepsilon_{ii}$ can be $\varepsilon_{xx}$, $\varepsilon_{yy}$, or $\varepsilon_{zz}$, $L_i$ is the initial length of the body in the $i$ direction, and $\Delta L_i$ is the corresponding change in this direction. Among them, the second and third terms are equal because under isotropic or homogeneous strains, the strain is constant over the material. Thirdly, to specifically describe the total volume change of the material, for example a cube, people introduce the scalar volumetric strain and approximate it as the sum of diagonal strain tensor components, which is shown by Eq. 4 in the manuscript. For Eq. 4, because the applied strain is small and isotropic, all high-order parts in the third term are ignored and linear strains along three directions are equal, as a result the volumetric strain can be approximated as $3\varepsilon$. Following this definition, we can easily define the volumetric strain for host and doped system by Eq. (5) and Eq. (6) in the manuscript.

## 3. Correction scheme for lattice strain

In this section, we present a method for correcting strain by linear fitting of calculated stress. We take the GaN crystal before doping as an example, and the correction after doping can be obtained similarly. First, taking VASP as an example, we select ISIF=3, repeatedly relax, and obtain a lattice close to the equilibrium position. Of course, we can also select ISIF=2 and obtain this lattice by fitting the equation of state. Then, taking this lattice as a reference, we apply a strain every 0.5% in the interval [-1.0%, 1.0%] and calculate its stress, the results are shown in FIG. S2(a). Next, based on the stress formula of the correction scheme in the main text, we make a linear fit for these five points, as shown in FIG. S2(b). Among them, the slope of the fitting line is the elastic coefficient of the system, and the intercept can be defined as the residual stress. Since the equilibrium state corresponds to zero stress, according to the ratio of the residual stress to the elastic coefficient, we obtain the strain deviation of the host crystal, -0.040. Then, substituting the strain deviation back into equations (5) and (7) in the main text, we can obtain the corrected equilibrium volume and the actual host strain, as shown in Table I in the main text. Finally, we can obtain the variation trend of the DFT-calculated lattice stress with the actual host strain, as shown in FIG. S2(c). Additionally, dopant atoms can change the elastic coefficients of the crystal by altering its atomic structure and bonding characteristics. Dopant atoms are usually different in types and atomic size from the host atoms. These differences can strengthen or weaken bonds in the local atomic environment, thereby altering the bond stiffness and magnitude of elastic coefficient.

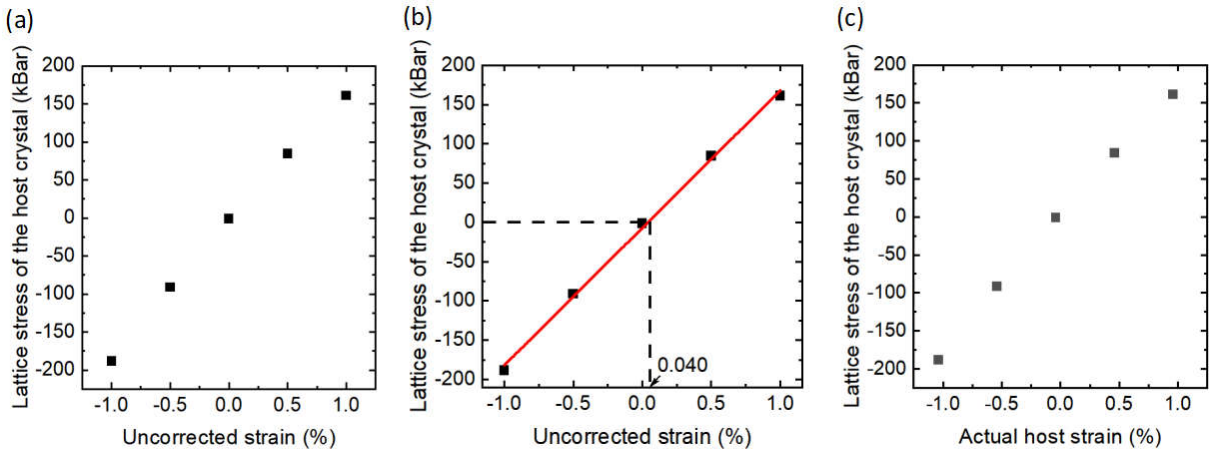


FIG. S2. (a) Lattice stress of the host crystal as a function of the uncorrected strain for GaN. (b) Linear fit of the lattice stress as a function of the uncorrected strain. The red line shows the fitting curve. The dashed lines are to show the determination of the strain deviation, -0.040, by using the zero stress condition. (c) Lattice stress of the host crystal as a function of the actual strain for GaN.

### 4. Definition of prediction deviation

In order to facilitate the comparison of prediction schemes before and after correction, in this section, we also need to define the prediction deviation of stress and formation energy. The steps are as follows. First, based on the equilibrium configuration after DFT relaxation, we apply a strain every 0.2% in the interval [-1.0%, 1.0%]. Then, based on DFT calculation, under strain, we can obtain the measured values of physical quantities such as the stress of the lattice before and after doping, the stress introduced by impurities, and the impurity formation energy. Then, after strain correction, we can obtain the predicted values of these quantities using equations (11), (13), (16), and (17) in the main text. Finally, the prediction deviation (PD) of stress or formation energy can be defined as,

$$PD = \frac{1}{n}\sum_{i=1}^{n}|X_i - X_i^{DFT}| \qquad \text{(S3)}$$

, where $X_i$ and $X_i^{DFT}$ correspond to the predicted value and DFT calculated value of the physical quantity under the i-th strain, respectively, n is the total number of selected strains, and $|X_i - X_i^{DFT}|$ defines the absolute deviation of the physical quantity under the i-th strain.

### 5. Comparison of $Ca_{Ga}$ and $V_N$ impurity-related local structures

In this section, in order to explain why the sum of the stress introduced by the size effect and the electron gas effect of the nitrogen vacancy does not match the overall stress, we analyze the local structure associated with $V_N$ and compare it with that of $Ca_{Ga}$. First, after doping $Ca_{Ga}$ and $V_N$ into GaN crystals, we obtain their respective local structures, as shown in FIG. S3(a) and (c). Then, in order to obtain an electrically neutral doping configuration, we add one electron and remove three electrons from the $Ca_{Ga}$ and $V_N$ doped crystals, respectively, the calculated results are shown in FIG. S3(b) and (d). In order to characterize the reconstruction, we list the average distance between the first nearest neighbor atoms of the impurity, and the results are shown in FIG. S3(g). We can see that compared with the unsaturated $V_N$, the average distance between the first nearest neighbor gallium atoms of the electrically neutral $V_N$ increases by about 20%. In $Ca_{Ga}$ doping, this is almost unchanged, and similar phenomena also exist in other substitutional impurities. For $V_N$ doping, the change in the average distance is because when three electrons are removed from the doping system, there are no electrons on the dangling bonds of these gallium atoms, so the reconstruction between gallium atoms in the neutral state is destroyed, resulting in a significant repulsion, which significantly increases the distance between gallium atoms. This highly localized additional coupling between gallium atoms cannot be effectively described by the electron gas model.

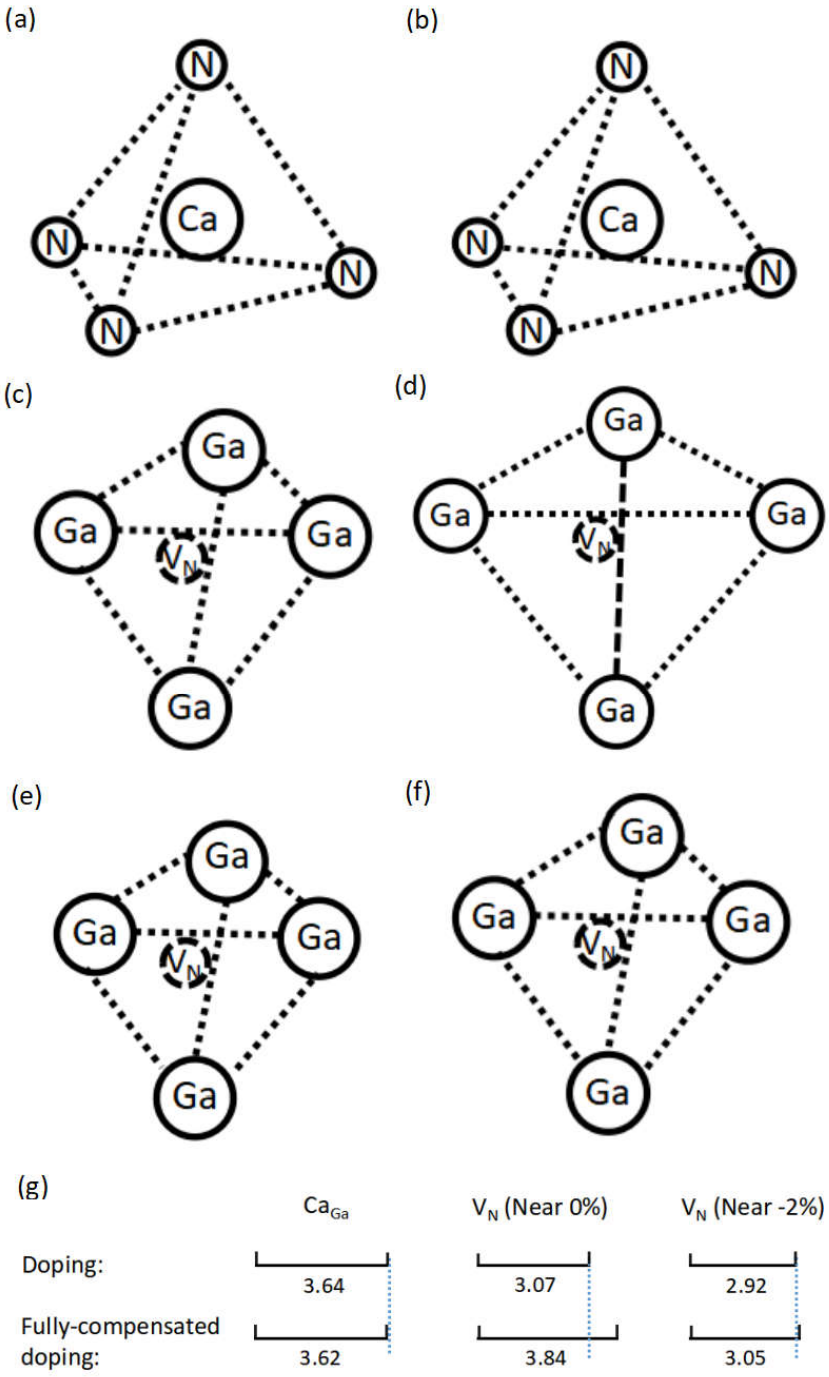


FIG. S3. (a) and (b) are illustrated structures for the $Ca_{Ga}$ in GaN before and after fully compensating near the strain of 0%, respectively. (c) and (d) are illustrated structures for the $V_N$ in GaN before and after fully compensating near the strain of 0%, respectively. (e) and (f) are illustrated structures for the $V_N$ in GaN before and after fully compensating near the strain of -2%, respectively. The $V_N$ is indicated by the dashed ball. The dotted line is to show the distance between the first nearest neighbors of the dopants. (g) A comparison of the average distances (Å) between the first nearest neighbors of the dopants, $Ca_{Ga}$ and $V_N$ of GaN, in the doping and fully compensated doping cases.

### 6. Response of dopant induced stress under large strains

To show the response in FIG. 4 over a larger strain range around [-2.0%, 2.0%], we have added FIG. S4. Generally, with the exception of the nitrogen vacancy in GaN, the response remains almost linear. The obvious nonlinearity of nitrogen vacancy in the fully compensated stress calculations near -2.0% reflects large local bonding reconstructions of Ga atoms around the vacancy under a large compressive strain, as shown in FIG. S3(d) and S3(f). Although three electrons are removed from the lattice, the neighboring Ga atoms still form bonds with a bond length of 3.05 Å, as shown in FIG. S3(g).

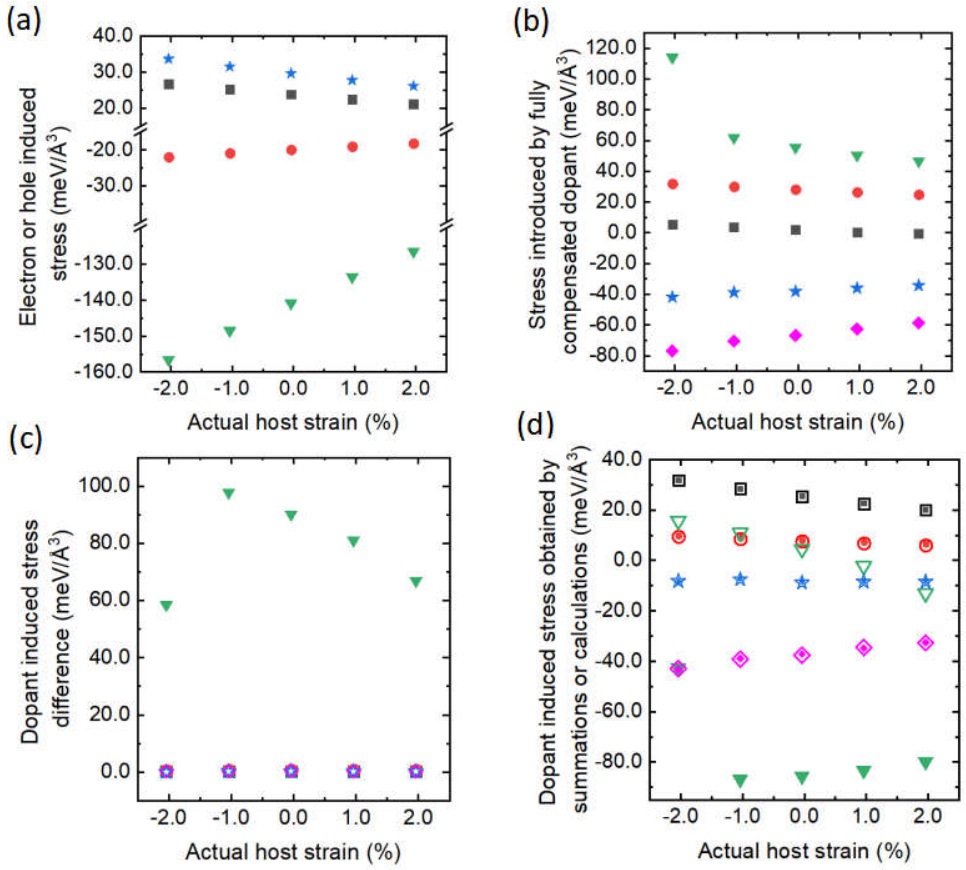


FIG. S4. (a) Electron or hole induced stress as a function of external strain. The black, red, blue and green points represent the introduction of one hole and one electron in silicon, and one hole and three electrons in GaN, respectively. (b) Stress introduced by fully compensated dopant as a function of external strain. (c) The difference between the summed dopant induced stress and the DFT-calculated dopant induced stress. (d) Dopant induced stress obtained by summations or DFT calculations as a function of external strain. Among (b), (c) and (d), the black, red, blue, purple, and green points correspond to the $B_{Si}$ and $P_{Si}$ in silicon, $Mg_{Ga}$, $Ca_{Ga}$ and nitrogen vacancy in GaN, respectively. Especially, in (d), the solid points represent summed stresses, and the hollow points represent DFT-calculated stresses.

**References**


1. Ahn, C., et al., Physical Review B, 2009. 79(7): p. 073201.
2. Zhu, J., et al., Physical Review Letters, 2010. 105(19): p. 195503.
3. Zhu, J., F. Liu, and M.A. Scarpulla, APL Materials, 2014. 2(1): p. 012110.
4. Yan, X., et al., Chinese Physics Letters, 2021. 38(8): p. 087103.
5. L. D. Landau, et al., Theory of Elasticity: Volume 7. (Butterworth-Heinemann, 2012), p. 3.
6. R. P. Feynman, et al., The Feynman Lectures on Physics, Vol. II: The New Millennium Edition: Mainly Electromagnetism and Matter. (Basic Books, 2011), p. 39-2.